

Reconstructing Jet Azimuthal Anisotropies with Cumulants

Tanner Mengel,^{1,2} Niseem Magdy,^{1,3,4} Ron Belmont,⁵ Anthony Timmins,⁶ and Christine Nattrass¹

¹*Department of Physics, University of Tennessee, Knoxville, TN, 37996, USA*

²*Department of Physics, University of Colorado, Boulder, Colorado 80309, USA*

³*Department of Physics, Texas Southern University, Houston, TX 77004, USA*

⁴*Physics Department, Brookhaven National Laboratory, Upton, New York 11973, USA*

⁵*Physics and Astronomy, University of North Carolina, Greensboro, North Carolina 27412, USA*

⁶*Department of Physics, University of Houston, Houston, Texas 77204, USA*

(Dated: January 16, 2026)

In relativistic heavy-ion collisions, where quark-gluon plasma forms, hadron production is anisotropic at both low and high transverse momentum, driven by flow dynamics and spatial anisotropies. To better understand these mechanisms, we use multi-particle correlations to reconstruct jet anisotropies. We simulate data using TENNEN as a hydro-like background and combine it with PYTHIA-8 generated jets, clustering them with the anti- k_t algorithm. Jet anisotropies are unfolded using a Bayesian technique, ensuring the robustness of the reconstructed signals. Our results demonstrate that multi-particle cumulant methods can accurately capture the differential jet azimuthal anisotropies, providing crucial insights into high- p_T behavior and the dynamics within heavy-ion collisions.

I. INTRODUCTION

Relativistic heavy-ion collisions create an extremely hot and dense phase of matter known as the quark-gluon plasma (QGP). Investigations at the Relativistic Heavy Ion Collider (RHIC) [1–4] and the Large Hadron Collider (LHC) [5–7] have demonstrated a wide array of complex phenomena related to the QGP. A key signature of QGP formation is the azimuthal anisotropy observed in the production of hadrons, particularly at low transverse momentum ($p_T < 3$ GeV). This anisotropy can be effectively modeled as hydrodynamic flow, with the final momentum distribution of hadrons reflecting initial spatial anisotropies, which are translated into momentum space through pressure gradients [8–14]. These azimuthal anisotropies are described using a Fourier expansion [15, 16]:

$$\frac{dN}{d\phi} \propto C \left[1 + 2 \sum_{n=1}^{\infty} v_n \cos(n(\phi - \psi_n)) \right] \quad (1)$$

where C is the normalization factor determined by the integral of the distribution, v_n and ψ_n denote the value and orientation for the anisotropy complex vector, respectively. In particular, v_2 and v_3 are called the elliptic and triangular coefficients, respectively.

At high transverse momentum ($p_T > 10$ GeV), hadron production in ion-ion (AA) collisions shows significant suppression compared to expectations based on proton-proton ($p + p$) collisions, a phenomenon understood as jet quenching [17, 18]. In this process, high-energy partons lose energy through both radiative and collisional interactions within the QGP [18–20]. These high- p_T hadrons and their associated jets also exhibit non-zero azimuthal anisotropy, even though they fall outside the

typical regime where the hydrodynamic flow would apply [21–23]. Instead, these anisotropies are understood to arise from the spatial inhomogeneities in the QGP, with jet quenching effects being more pronounced for partons traveling through longer paths in the QGP [24–26]. The pathlength is minimized when ϕ and ψ_n are approximately aligned, leading to less jet attenuation. In contrast, when ϕ and ψ_n are approximately orthogonal, the pathlength is maximized, which leads to increased jet attenuation.

Both low- and high- p_T hadrons share a standard orientation of their anisotropies, correlating with the geometry of the colliding nucleons. A long-standing theoretical challenge has been to simultaneously explain both high- p_T suppression and the corresponding azimuthal anisotropy observed in A+A collisions, and several models have been proposed to address this issue [25, 27–32]. Previous measurements of jet differential azimuthal anisotropies v_n^{jet} have used an event plane method where the event plane is defined by soft particles [22, 33, 34]. Given observations in the soft sector, these jet anisotropy coefficients should also be sensitive to the measurement technique. Some studies indicate that the difference could be up to 10% [35–37], which is on the order of the uncertainty on measurements by ATLAS [38].

Measurements from smaller collision systems, such as $p + p$ and $p+\text{Pb}$ at the LHC [39–44], and $p+\text{Au}$, $d+\text{Au}$, and $^3\text{He}+\text{Au}$ at RHIC [45, 46], have also revealed significant azimuthal anisotropies at low- p_T , with patterns similar to those observed in heavy-ion collisions. These findings suggest that even smaller systems may produce short-lived droplets of the QGP; indeed, hydrodynamic models have successfully described the low- p_T behavior in such systems. However, when it comes to high- p_T behavior in smaller collision systems, the expected signatures of jet quenching have not been observed. While some

measurements indicate that no jet suppression at high transverse momentum in $p+\text{Pb}$ and $d+\text{Au}$ collisions [47–50], other studies indicate there may be some suppression [51]. No alterations in the momentum balance of dijets or hadron-jet pairs have been detected.

The ATLAS experiment has also reported non-zero azimuthal anisotropies for hadrons with p_T up to 12 GeV, suggesting an extension of anisotropy effects into the high- p_T regime typically associated with jet quenching. It is unclear if differential jet quenching contributes to the observed high- p_T anisotropies [49]. This leaves two related unresolved puzzles: the lack of jet quenching observed in $p+A$ collisions and the mechanism that produces high- p_T hadron anisotropies in the absence of jet quenching.

Further investigation into the mechanism responsible for high- p_T hadron anisotropies requires two key approaches: (i) comparing data models with both theory and experiment using consistent techniques and (ii) expanding measurements to incorporate multi-particle correlations. Discrepancies between event plane and cumulant methods can reach up to 10% [35–37, 52]. These variations can complicate the interpretation of experimental measurements made with the event plane method. Several factors, such as long-range non-flow effects and initial/final state fluctuations, can influence the flow correlations measured with the 2-particle correlation method, potentially amplifying the observed flow signal. Therefore, applying 2- and multi-particle cumulant methods in data analysis and theoretical calculations is crucial for a deeper understanding of the mechanisms behind high- p_T hadron anisotropies.

In this work, we demonstrate the feasibility of measuring the jet azimuthal anisotropies v_n^{jet} with 2- and 4-particle cumulants in $\text{Au}+\text{Au}$ collisions simulated with PYTHIA-8 [53, 54] jets merged with a TENNGEN [55–57] background.

II. METHOD

A. Simulation

Events are simulated in TENNGEN [55, 57, 58], a data-driven background generator designed to reproduce correlations arising from flow. In this model, the n^{th} -order event plane is set to zero for even values of n , while for odd values of n , the event plane is chosen randomly. TENNGEN multiplicities and charged particle ratios match experimentally measured values [59, 60]. Similar constraints are also applied to the transverse momentum spectra of charged pions, kaons, and protons through random sampling from an initial distribution fitted to a Blast Wave [61, 62] distribution. In TENNGEN, the generated particle $v_n(\eta)$ is sampled from a flat distribution, an acceptable approximation for the region $|\eta| < 1.1$. The single particle $v_n(p_T)$ are modeled using a polynomial fit to the measured $v_n(p_T)$ [63, 64]. TEN-

NGEN events used in this study are tuned to $\text{Au}+\text{Au}$ collision data at $\sqrt{s_{\text{NN}}} = 200$ GeV for 20–30% central events. TENNGEN serves as a hydro-like background for jet interactions. The jet signal is generated using PYTHIA-8 [54] with the Monash Tune 13 [65] and a minimum hard scattering transverse momentum cutoff of $\hat{p}_T^{\text{min}} > 5$ GeV.

The leading PYTHIA jets are realigned to simulate a $\frac{dN_{\text{jet}}}{d\phi_{\text{jet}}}$ distribution with non-zero differential azimuthal anisotropies v_n^{jet} . Previous measurements of v_n^{jet} by the ATLAS collaboration indicate there may be a nonzero dependence on jet p_T [22, 33, 38]. To ensure our method is robust to such dependence, we consider several functional forms to model a wide range of momentum dependence on the jet azimuthal anisotropies $v_n^{\text{jet}}(p_T)$. These include three p_T independent constant values of v_n^{jet} , a $v_n^{\text{jet}}(p_T)$ which increases with p_T , and a physically unrealistic sinusoidal dependence on p_T . We are confident that any expected dependence of v_n^{jet} on jet p_T in experimental data will be less extreme than the latter. Leading PYTHIA jets are realigned to simulate nonzero v_2^{jet} , v_3^{jet} , and v_4^{jet} according to one of the following descriptions:

$$\begin{aligned} v_n^{\text{jet}} &= \alpha_n, \\ v_n^{\text{jet}} &= 2\alpha_n, \\ v_n^{\text{jet}} &= 5\alpha_n, \\ v_n^{\text{jet}} &= \alpha_n + \frac{\beta}{2}p_T, \\ v_n^{\text{jet}} &= \alpha_n [2 + \cos \beta p_T], \end{aligned} \quad (2)$$

where α_n is a nominal scale for each harmonic n , and β is constant parameter for all n . The values used in this study are $a_2 = 4\%$, $a_3 = 1\%$, $a_4 = 0.5\%$, and $\beta = 0.2$. Figure 1 shows the five v_n^{jet} used in the realignment of leading PYTHIA jets. A total of 10 million TENNGEN +PYTHIA-8 events are generated for each sample. The simulation package developed to generate these events is publicly available [?].

The merged PYTHIA-8 jet constituents and TENNGEN charged particles are clustered into anti- k_T jets with jet resolution parameter $R = 0.4$ using the energy recombination scheme implemented with FASTJET-3 [66]. The charged final-state hadrons from PYTHIA-8 $p+p$ events are clustered separately before merging with TENNGEN, which defines the truth jet momentum. The $p+p$ event is used if there is at least one jet with $p_{T,\text{jet}} > 10$ GeV. Ghost particles with $p_T^{\text{ghost}} = 1$ MeV are used to estimate the area of clustered merged jets as described in the FastJet manual [66].

The momentum of the merged jets is corrected using the jet-multiplicity background subtraction method [56]

$$p_{T,\text{jet}}^{\text{corr, N}} = p_{T,\text{jet}}^{\text{raw}} - \rho_{\text{mult}}(N_{\text{tot}} - \langle N_{\text{sig}} \rangle), \quad (3)$$

where N_{tot} is the observed number of particles within the jet, $\langle N_{\text{sig}} \rangle$ is approximated by the average number of PYTHIA-8 particles in a TENNGEN +PYTHIA-8 jet of a given matched uncorrected jet momentum bin, and

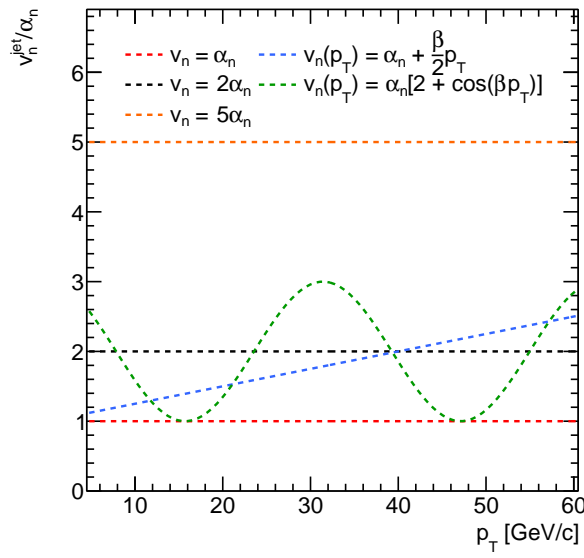


FIG. 1. The dependence of v_n^{jet} on jet p_T for functions used to realign leading PYTHIA jets in PYTHIA-8 + TENGGEN events. These include three p_T independent constant values of v_n^{jet} (red, black, and orange dotted lines), a $v_n^{\text{jet}}(p_T)$ which increases with p_T (blue dotted line), and a physically unrealistic sinusoidal dependence on p_T (green dotted line). The y -axis is scaled by a_n .

ρ_{Mult} is the mean transverse momentum per background particle. Merged jet candidates satisfying $p_{T,jet}^{\text{corr}} > 5$ GeV and $A_{\text{jet}} > 0.6\pi R^2$ [67] are geometrically matched back to the jet axis of the PYTHIA-8 signal jet. The closest merged jet is considered a match if $\Delta R < 0.75R$ and the corresponding PYTHIA-8 jet momentum $p_{T,jet}^{\text{PYTHIA}}$ is taken to be the truth momentum.

B. Cumulant Method

The traditional cumulant method [68, 69], is used to construct the $v_n\{2k\}(p_T)$, where k is a positive integer. In this work, the $v_n^{\text{jet}}\{2k\}$ is given as:

$$\begin{aligned} v_n^{\text{jet}}\{2\} &= \frac{\langle\langle 2'_n \rangle\rangle}{\langle\langle 2_n \rangle\rangle^{1/2}}, \\ \langle\langle 2'_n \rangle\rangle &= \langle\langle e^{in(\psi_1^A - \varphi_2^C)} \rangle\rangle, \\ \langle\langle 2_n \rangle\rangle &= \langle\langle e^{in(\varphi_1^C - \varphi_2^C)} \rangle\rangle, \end{aligned} \quad (4)$$

$$\begin{aligned} v_n^{\text{jet}}\{4\} &= \frac{\langle\langle 4'_n \rangle\rangle}{(-\langle\langle 4_n \rangle\rangle)^{3/4}}, \\ \langle\langle 4'_n \rangle\rangle &= \langle\langle e^{in(\psi_1^A + \varphi_2^C - \varphi_3^C - \varphi_4^C)} \rangle\rangle \\ &\quad - 2 \langle\langle e^{in(\varphi_1^C - \varphi_2^C)} \rangle\rangle \langle\langle e^{in(\psi_1^A(p_T) - \varphi_2^C)} \rangle\rangle, \\ \langle\langle 4_n \rangle\rangle &= \langle\langle e^{in(\varphi_1^C + \varphi_2^C - \varphi_3^C - \varphi_4^C)} \rangle\rangle \\ &\quad - 2 \langle\langle e^{in(\varphi_1^C - \varphi_2^C)} \rangle\rangle \langle\langle e^{in(\varphi_1^C - \varphi_2^C)} \rangle\rangle, \end{aligned} \quad (5)$$

where φ^C is the azimuthal angle of particles in the region C , ψ^A is the azimuthal angle of jets in the region A , and $\langle\langle 2_n \rangle\rangle$ is the event averaged 2-particle correlations of order n . The prime ('') symbol is used to differentiate the particle of interest correlation from the reference correlation. The integrated φ is taken from particles labeled as reference flow particles in region C with $3.1 < |\eta_C| < 5.1$. The ψ is the particle of interest (i.e., jet) azimuthal angle defined within region A with $|\eta_A| < 1.1 - R$. More details about the traditional cumulant method can be found in Appendix A.

The differential azimuthal anisotropies for jets $v_n^{\text{jet}}\{2k\}$ are binned as a function of uncorrected jet momentum. Jet measurements with p_T dependencies are subject to bin-by-bin migration from smearing due to finite resolution in the uncorrected measurement. This smearing can skew the event-averaged differential particle correlations if the functional form of v_n^{jet} is dependent on jet momentum. If the v_n^{jet} are independent of jet momenta, then this smearing will not change the results. Measurements of v_n^{jet} indicate there may be a nonzero dependence on $p_{T,\text{jet}}$, meaning that measurements using a cumulant method will need to be unfolded [22, 33, 38].

We unfold the reconstructed differential single-event n^{th} -order $2k$ -particle correlations using the Bayesian unfolding method [70] in ROOUNFOLD 2.0.0 [71]. From Equations 4 5, we define the single-event n^{th} -order $2k$ -particle correlations, for use in constructing a response matrix. That is

$$\begin{aligned} \langle 2_n \rangle &= \langle e^{in(\varphi_1^C - \varphi_2^C)} \rangle, \\ \langle 2'_n \rangle &= \langle e^{in(\psi_1^A - \varphi_2^C)} \rangle, \end{aligned} \quad (6)$$

$$\begin{aligned} \langle 4_n \rangle &= \langle e^{in(\varphi_1^C + \varphi_2^C - \varphi_3^C - \varphi_4^C)} \rangle - 2 \langle 2_n \rangle^2, \\ \langle 4'_n \rangle &= \langle e^{in(\psi_1^A + \varphi_2^C - \varphi_3^C - \varphi_4^C)} \rangle - 2 \langle 2_n \rangle \langle 2'_n \rangle, \end{aligned} \quad (7)$$

where φ^C is the azimuthal angle of particles in the region C , ψ^A is the azimuthal angle of jets in the region A , binned in reconstructed jet p_T . Again, the prime ('') symbol is used to differentiate the jet azimuthal correlations from the reference particle correlations.

PYTHIA-8 jets (truth jets) are matched to PYTHIA-8 + TENGGEN jets (reconstructed jets) and the momentum and azimuthal angle of the PYTHIA-8 jet is taken as the truth momentum ($p_{T,jet}^{\text{truth}}$) and truth azimuthal angle ($\phi_{jet}^{\text{truth}}$). A reconstructed-level jet is considered a match to the closest truth-level jet in η, ϕ space if the separation is $dR < \frac{3}{4}R$. From the matched truth jet, the truth-level single event correlation $\langle\langle (2k)_n \rangle\rangle^{\text{truth}}$ is calculated. There are no matching criteria imposed between the reconstructed-level $\langle\langle (2k)_n \rangle\rangle^{\text{reco}}$ and the truth-level $\langle\langle (2k)_n \rangle\rangle^{\text{truth}}$. Both single-event correlations are calculated using the same $p_{T,jet}$ binning with a bin-width of 5 GeV.

We construct a four-dimensional response matrix, populated for bin migration of the yield as a function of the reconstructed-level $\langle\langle (2k)_n \rangle\rangle^{\text{reco}} \otimes p_{T,jet}^{\text{reco}}$ and the matched

truth-level $\langle (2k)'_n \rangle^{\text{truth}} \otimes p_{T,jet}^{\text{truth}}$. We then unfold our reconstructed jet differential single-event n^{th} -order $2k$ -particle correlations. The unfolding procedure is repeated until the change in χ^2 between the unfolded and truth $\langle (2k)'_n \rangle$ becomes less than the uncertainties of the measured $\langle (2k)'_n \rangle$. This typically occurs between 3-5 iterations, and more iterations beyond this threshold would yield diminishing increases in unfolded $\langle (2k)'_n \rangle$ resolution. The average value of the resulting unfolded single-event correlation is $\langle (2k)'_n \rangle^{\text{corr}}$ is calculated for each jet momentum bin and used to compute $v_n^{\text{jet}}(p_T)$, according to Equations 4- 5.

To demonstrate the robustness of this procedure, we unfold $\langle (2k)'_n \rangle^{\text{reco}}$ corresponding to a p_T independent v_n^{jet} with response matrices constructed from models with different functional forms. The results of this exercise are presented in Figure 2. We show that the corrected $v_n^{\text{jet,corr}}\{2k\}(p_T)$ recovers the functional form of a given model, regardless of the functional form present in the construction of the response matrix.

III. RESULTS

The simulated data using PYTHIA-8 +TENNGEN are analyzed using the 2- and 4-particle cumulant methods with several input flow signals. We present the $v_n^{\text{jet}}\{2\}$ for several $p_{T,jet}$ selection for Au+Au at 200 GeV in Figure 3. The input $v_{n,\text{jet}}^{\text{jet,MC}}$ is a constant equal to 0.08, 0.02, and 0.01 for $n = 2, 3$ and 4, respectively. The $v_n^{\text{jet,corr}}\{2k\}$ are obtained after five iterations of Bayesian unfolding. Our results reflect the capabilities of using the 2-particle cumulant method to reflect the input jet v_n^{jet} . The presented results also reflected the input sensitivity to the flow harmonic order attenuation.

Extending our analysis to the 4-particle cumulant will offer deeper insights into the impact of flow fluctuations on jet flow measurements, as well as the effects of short- and long-range correlations. In this context, short-range correlations primarily arise from localized effects, such as particle decays or intra-jet correlations [72–77]. These contributions can be mitigated by applying multi-particle sub-event cumulant methods.

Figure 4 presents the corrected $v_2^{\text{jet}}\{2k\}$ (where $k = 1$ or 2 for the 2- and 4-particle correlation, respectively) as a function of $p_{T,jet}$ for various functional forms of $v_n^{\text{jet,MC}}$. These forms encompass different realistic scenarios where v_n^{jet} remains either independent of or gradually increases with $p_{T,jet}$, as well as physically unrealistic forms, such as $v_n^{\text{jet}} \propto \cos(p_{T,jet})$. The inclusion of both realistic and unrealistic models underscores the robustness of our method in reconstructing differential jet azimuthal anisotropies, even under extreme conditions. Furthermore, our results indicate an agreement between $v_2^{\text{jet}}\{2\}$ and $v_2^{\text{jet}}\{4\}$, reflecting the model’s nature, which lacks flow fluctuations effects.

IV. CONCLUSIONS

This work demonstrates the utility of 2- and 4-particle cumulant methods for measuring jet anisotropies, leveraging TennGen and PYTHIA models to simulate data representative jet backgrounds in the quark-gluon plasma. Our findings demonstrate that cumulants can be effectively used to reconstruct jet azimuthal anisotropies, capturing their flow characteristics and providing a robust means to analyze high- p_T jet azimuthal anisotropies. This methodology offers promise for disentangling long and short-range correlations between jets. Since it is not possible to reconstruct an event plane in small systems this technique can be used to advance the understanding of jet interactions and anisotropies in heavy-ion and smaller collision systems.

In real heavy-ion collisions, there are several effects, such as uncorrelated jets and resonance decays. These effects could be significant in small systems, and would have to be considered in order to properly interpret the results. Additionally, event-by-event flow fluctuations will contribute to differences in different order cumulants. In A+A systems, where the relative fluctuations are mostly small, $v_2\{2\} = \sqrt{v_2^2 + \sigma^2}$ and $v_2\{4\} \approx v_2\{6\} \approx v_2\{8\} \approx \sqrt{v_2^2 - \sigma^2}$. However, in small systems, the relative fluctuations can be large, and the nature of the underlying distribution becomes important. Addressing these effects will be important for ensuring the applicability of this method to experimental data.

V. ACKNOWLEDGMENTS

This work was supported in part by funding from the Division of Nuclear Physics of the U.S. Department of Energy under Grant No. DE-FG02-96ER40982. This work was performed on the computational resources at the Infrastructure for Scientific Applications and Advanced Computing (ISAAC) supported by the University of Tennessee.

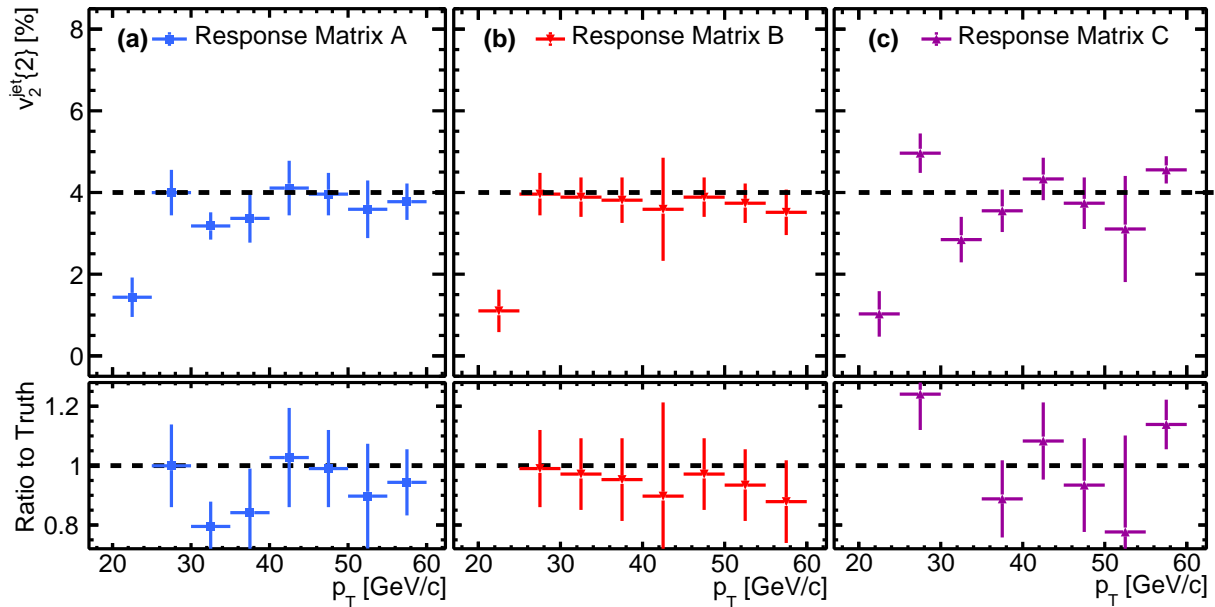


FIG. 2. Comparisons of the $v_2^{\text{jet}}\{2\}$ calculated with unfolded $\langle 2'_2 \rangle^{\text{corr}}$ for PYTHIA-8 + TENGGEN events with a p_T independent truth $v_2^{\text{jet}} = 4\%$, unfolded with response matrices constructed from PYTHIA-8 + TENGGEN events where $v_2^{\text{jet}} = 4\%$ (Response Matrix A), a scaled constant $v_2^{\text{jet}} = 5 \times 4\%$ (Response Matrix B), and a linear p_T dependence $v_2^{\text{jet}}(p_T) = 4\% + (0.1\%) \times p_T$ (Response Matrix C). The dashed line represents the true constant $v_2^{\text{jet}} = 4\%$ of the unfolded sample.

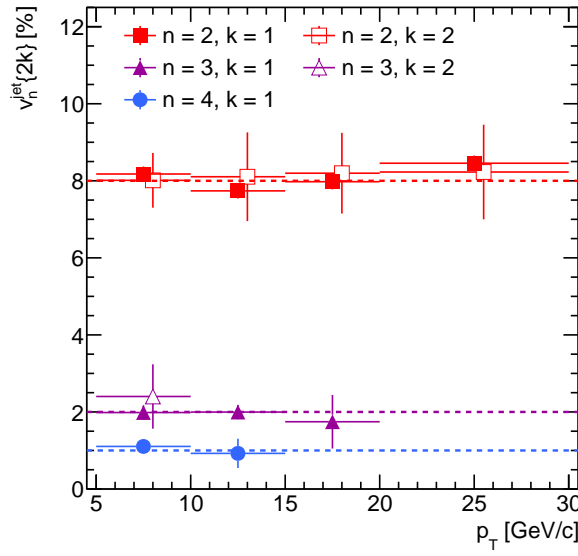


FIG. 3. The p_T dependence of $v_n^{\text{jet}}\{2k\}$ for harmonic order $n = 2, 3$, and 4 , represented by the red squares, purple triangles, and blue circles, respectively. Values calculated using 2- and 4-particle correlations are differentiated by full ($k = 1$) or open ($k = 2$) symbols. The dashed line represents the true $v_n^{\text{jet}}(p_T)$ values.

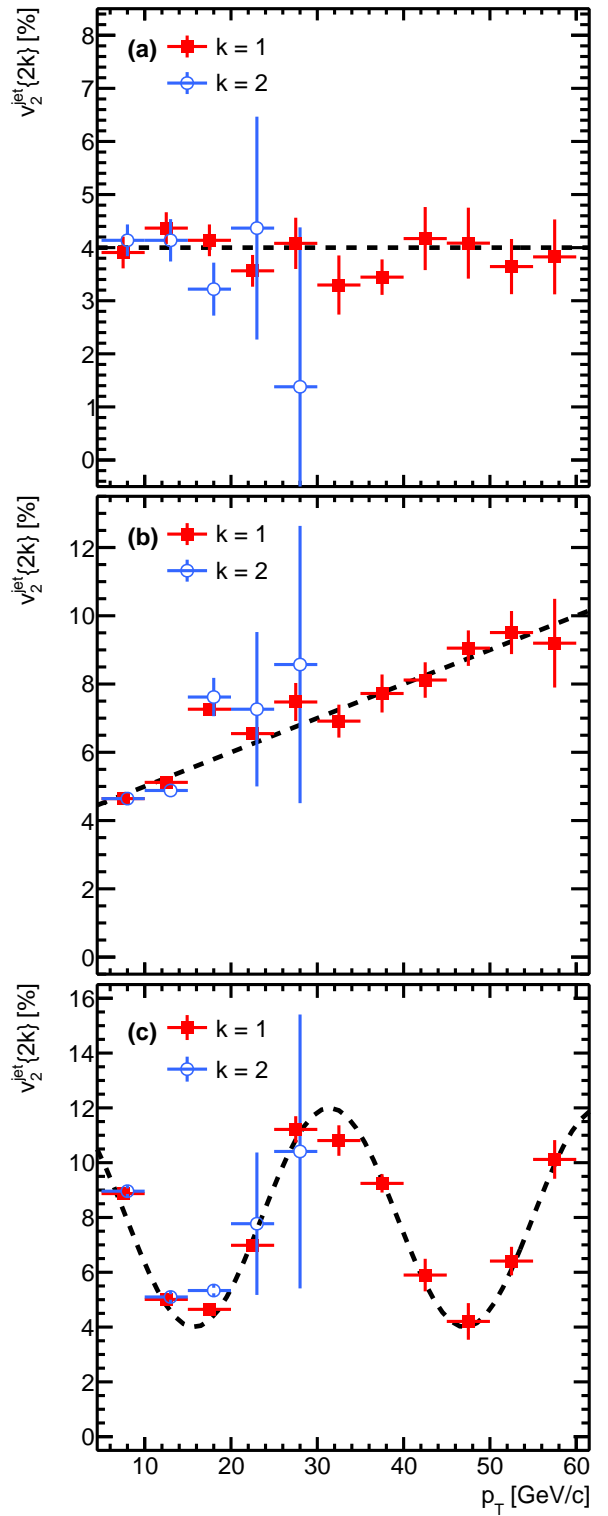


FIG. 4. Comparison of the p_T dependence of the $v_2^{\text{jet}}\{2k\}$ for Au+Au collisions at 200 GeV calculated with 2-particle ($k = 1$) and 4-particle ($k = 2$) correlations. The dashed line represents the true $v_n^{\text{jet}}(p_T)$ values. The unfolded $v_2^{\text{jet}}\{2k\}$ $v_2^{\text{jet}} = 4\%$ (a), a linear p_T dependence $v_2^{\text{jet}}(p_T) = 4\% + (0.1\%) \times p_T$ (b), and a sinusoidal p_T dependence $v_n^{\text{jet}} = 4\% \times [2 + \cos 0.2p_T]$ (c).

Appendix A: Additional Cumulant Method Details

We use the method presented in [68] which calculates multi-particle cumulants in terms of moments of \mathbf{Q} vectors defined as

$$\mathbf{Q}_n \equiv \sum_{k=1}^M e^{in\phi_k}, \quad (\text{A1})$$

where M is the multiplicity of the referenced sub-event and ϕ_k is the azimuthal angle of particles labeled as Reference Flow Particles (RFP). We define our sub-event region as being away from mid-rapidity, $3.1 < |\eta| < 5.1$. For this study, we simulate events with M fixed at 363. This M corresponds to an average 20-30% central Au+Au $\sqrt{s_{NN}} = 200$ GeV collision [59]. We use a single bracket to denote average moments of Equation A1 $\langle 2k_n \rangle$, which are averaged over all M and double brackets to denote event-averaged moments $\langle\langle (2k)_n \rangle\rangle$ which are averaged over all events. Using moments of Equation A1, the single event n^{th} -order 2- and 4-particle reference azimuthal correlations can be expressed as

$$\langle 2_n \rangle = \frac{|\mathbf{Q}_n|^2 - M}{M(M-1)}, \quad (\text{A2})$$

and

$$\begin{aligned} \langle 4_n \rangle = & \frac{|\mathbf{Q}_n|^2 + |\mathbf{Q}_{2n}|^2 - 2\Re\{\mathbf{Q}_{2n}\mathbf{Q}_n^*\mathbf{Q}_n^*\}}{M(M-1)(M-2)(M-3)} \\ & - 2 \frac{(M-2)|\mathbf{Q}_n|^2 - M(M-3)}{M(M-1)(M-2)(M-3)}, \end{aligned} \quad (\text{A3})$$

where $|\mathbf{Q}_n|^2$ is the squared magnitude of \mathbf{Q} , \mathbf{Q}_{2n} is the \mathbf{Q} -vector for $n = 2n$, $\Re\{\cdot\}$ is the real component of the complex argument and M is the reference multiplicity. The event averaged n^{th} -order $2k$ -particle reference azimuthal correlation $\langle\langle (2k)_n \rangle\rangle$ is computed with a weighted sum of the single event reference azimuthal correlation

$$\langle\langle (2k)_n \rangle\rangle = \frac{1}{W\{2k\}} \sum_{i=1}^{N_{\text{events}}} (w\{2k\})_i \langle\langle (2k)_n \rangle\rangle_i, \quad (\text{A4})$$

where $(w\{2k\})_i$ are event weights and $W\{2k\}$ is the sum of all event weights. Common choices for weights are reference multiplicity or particle momentum. In the case when the multiplicity of the reference is limited, methods for momentum weighting are outlined in [68]. In our model, M is fixed, and the v_n of TennGen is independent of multiplicity. Therefore we use the weights

$$\begin{aligned} w\{2\} &= M(M-1), \\ w\{4\} &= M(M-1)(M-2)(M-3), \end{aligned} \quad (\text{A5})$$

for 2- and 4-particle RFP correlations respectively.

The second-order cumulant for the reference sub-event is defined as

$$c_n\{2\} \equiv \langle\langle 2_n \rangle\rangle, \quad (\text{A6})$$

which is simply the event averaged n^{th} -order 2-particle reference azimuthal correlation defined in Equation A2. The fourth-order reference cumulant is given by

$$c_n\{4\} \equiv \langle\langle 4_n \rangle\rangle - 2 \cdot \langle\langle 2_n \rangle\rangle^2, \quad (\text{A7})$$

which is the n^{th} -order 4-particle reference azimuthal correlation corrected for event-by-event fluctuations in the n^{th} -order 2-particle reference azimuthal correlation.

The differential single event azimuthal correlation for jets with respect to the reference correlation is calculated using additional flow vector \mathbf{p} , as well as the reference flow vector \mathbf{Q} defined in Equation A1. To measure the jet v_n , the Point of Interest (POI) vector \mathbf{p} is built using the azimuthal angle of all jets in an event within $|\eta_{\text{jet}}| < 1.1 - R$, defined as

$$\mathbf{p}_n \equiv \sum_{k=1}^{m_p} e^{in\psi_k}, \quad (\text{A8})$$

where m_p is the number of jets within a given p_T bin in an event and ψ_k is the azimuthal angle of the jet axis.

The n^{th} -order 2- and 4-particle differential single event azimuthal correlations are expressed as

$$\langle 2'_n \rangle = \frac{\mathbf{p}_n \mathbf{Q}_n^*}{m_p M}, \quad (\text{A9})$$

and

$$\langle 4'_n \rangle = \frac{(|\mathbf{Q}_n|^2 - 2M + 2)\mathbf{p}_n \mathbf{Q}_n^* - \mathbf{p}_n \mathbf{Q}_n \mathbf{Q}_{2n}^*}{m_p M(M-1)(M-2)}, \quad (\text{A10})$$

where m_p is the number of jets within a given p_T bin in an event, and \mathbf{p}_n is the POI vector. The event averaged n^{th} -order $2k$ -particle reference differential azimuthal correlation $\langle\langle (2k)'_n \rangle\rangle$ is computed similar to Equation A4 with the corresponding weights

$$\begin{aligned} w'\{2\} &= m_p M, \\ w'\{4\} &= m_p M(M-1)(M-2), \end{aligned} \quad (\text{A11})$$

for the differential 2- and 4-particle azimuthal correlations respectively.

These definitions for $\langle 2'_n \rangle$ and $\langle 4'_n \rangle$ differ slightly from the standard n^{th} -order 2- and 4-particle differential single event azimuthal correlations [68] due to the fact that we do not have to consider points which are labeled as both RFP and POI because the azimuthal angle of the jet axis ψ_{jet} is a composite angle from recombination of particles using a jet clustering algorithm. In practice, for jet v_n , it may be necessary to use RFP and POI correlations in different rapidity regions in order to avoid autocorrelations from using jet constituents in the RFP.

From the definitions for $\langle 2'_n \rangle$ and $\langle 4'_n \rangle$, the second and fourth order POI cumulants can be defined as

$$d_n\{2\} \equiv \langle\langle 2'_n \rangle\rangle, \quad (\text{A12})$$

and

$$d_n\{4\} \equiv \langle\langle 4'_n \rangle\rangle - 2 \cdot \langle\langle 2'_n \rangle\rangle \langle\langle 2_n \rangle\rangle, \quad (\text{A13})$$

where $d_n\{2\}$ is the the n^{th} -order 2-particle average differential azimuthal correlation and $d_n\{4\}$ is the n^{th} -order 4-particle differential azimuthal correlation corrected for event-by-event fluctuations.

The reference azimuthal anisotropies are calculated from the reference cumulants $c_n\{2k\}$ defined in Equations A6 A7

$$v_n\{2\} \equiv \sqrt{c_n\{2\}}, \quad (\text{A14})$$

and

$$v_n\{4\} \equiv \sqrt[4]{-c_n\{4\}}, \quad (\text{A15})$$

where $v_n\{2\}$ and $v_n\{4\}$ are used to denote estimations of the integrated flow v_n using the 2nd and 4th-order cumulants respectively.

The differential jet azimuthal anisotropies $v_n^{\text{jet}}\{2k\}$ are calculated using the differential cumulants $d_n\{2k\}$ defined in Equations A12 A13 with respect to the the reference azimuthal anisotropies $v_n\{2k\}$

$$v_n^{\text{jet}}\{2\}(p_T) = \frac{d_n\{2\}(p_T)}{v_n\{2\}}, \quad (\text{A16})$$

$$v_n^{\text{jet}}\{4\}(p_T) = -\frac{d_n\{4\}(p_T)}{(v_n\{4\})^{3/4}}, \quad (\text{A17})$$

where $v_n^{\text{jet}}\{2\}(p_T)$ and $v_n^{\text{jet}}\{4\}(p_T)$ are used to denote estimations of the differential flow for jets with a given transverse momentum p_T using the 2nd and 4th-order differential cumulants respectively.

[1] J. Adams *et al.* (STAR), Experimental and theoretical challenges in the search for the quark gluon plasma: The STAR Collaboration's critical assessment of the evidence from RHIC collisions, *Nucl. Phys. A* **757**, 102 (2005), arXiv:nucl-ex/0501009.

[2] K. Adcox *et al.* (PHENIX), Formation of dense partonic matter in relativistic nucleus-nucleus collisions at RHIC: Experimental evaluation by the PHENIX collaboration, *Nucl. Phys. A* **757**, 184 (2005), arXiv:nucl-ex/0410003.

[3] I. Arsene *et al.* (BRAHMS), Quark gluon plasma and color glass condensate at RHIC? The Perspective from the BRAHMS experiment, *Nucl. Phys. A* **757**, 1 (2005), arXiv:nucl-ex/0410020.

[4] B. B. Back *et al.* (PHOBOS), The PHOBOS perspective on discoveries at RHIC, *Nucl. Phys. A* **757**, 28 (2005), arXiv:nucl-ex/0410022.

[5] S. Acharya *et al.* (ALICE), The ALICE experiment: a journey through QCD, *Eur. Phys. J. C* **84**, 813 (2024), arXiv:2211.04384 [nucl-ex].

[6] A. Hayrapetyan *et al.* (CMS), Overview of high-density QCD studies with the CMS experiment at the LHC, *Phys. Rept.* **1115**, 219 (2025), arXiv:2405.10785 [nucl-ex].

[7] W. Busza, K. Rajagopal, and W. van der Schee, Heavy Ion Collisions: The Big Picture, and the Big Questions, *Ann. Rev. Nucl. Part. Sci.* **68**, 339 (2018), arXiv:1802.04801 [hep-ph].

[8] T. Hirano, U. W. Heinz, D. Kharzeev, R. Lacey, and Y. Nara, Hadronic dissipative effects on elliptic flow in ultrarelativistic heavy-ion collisions, *Phys. Lett. B* **636**, 299 (2006), arXiv:nucl-th/0511046.

[9] P. Huovinen, P. F. Kolb, U. W. Heinz, P. V. Ruuskanen, and S. A. Voloshin, Radial and elliptic flow at RHIC: Further predictions, *Phys. Lett. B* **503**, 58 (2001), arXiv:hep-ph/0101136.

[10] T. Hirano and K. Tsuda, Collective flow and two pion correlations from a relativistic hydrodynamic model with early chemical freezeout, *Phys. Rev. C* **66**, 054905 (2002), arXiv:nucl-th/0205043.

[11] P. Romatschke and U. Romatschke, Viscosity Information from Relativistic Nuclear Collisions: How Perfect is the Fluid Observed at RHIC?, *Phys. Rev. Lett.* **99**, 172301 (2007), arXiv:0706.1522 [nucl-th].

[12] H. Song, S. A. Bass, U. Heinz, T. Hirano, and C. Shen, 200 A GeV Au+Au collisions serve a nearly perfect quark-gluon liquid, *Phys. Rev. Lett.* **106**, 192301 (2011), [Erratum: *Phys. Rev. Lett.* 109, 139904 (2012)], arXiv:1011.2783 [nucl-th].

[13] B. Schenke, S. Jeon, and C. Gale, Anisotropic flow in $\sqrt{s} = 2.76$ TeV Pb+Pb collisions at the LHC, *Phys. Lett. B* **702**, 59 (2011), arXiv:1102.0575 [hep-ph].

[14] R. A. Lacey, D. Reynolds, A. Taranenko, N. N. Ajitanand, J. M. Alexander, F.-H. Liu, Y. Gu, and A. Mwai, Acoustic scaling of anisotropic flow in shape-engineered events: implications for extraction of the specific shear viscosity of the quark gluon plasma, *J. Phys. G* **43**, 10LT01 (2016), arXiv:1311.1728 [nucl-ex].

[15] S. Voloshin and Y. Zhang, Flow study in relativistic nuclear collisions by Fourier expansion of Azimuthal particle distributions, *Z. Phys. C* **70**, 665 (1996), arXiv:hep-ph/9407282.

[16] A. M. Poskanzer and S. A. Voloshin, Methods for analyzing anisotropic flow in relativistic nuclear collisions, *Phys. Rev. C* **58**, 1671 (1998), arXiv:nucl-ex/9805001.

[17] M. Connors, C. Nattrass, R. Reed, and S. Salur, Jet measurements in heavy ion physics, *Rev. Mod. Phys.* **90**, 025005 (2018), arXiv:1705.01974 [nucl-ex].

[18] G.-Y. Qin and X.-N. Wang, Jet quenching in high-energy heavy-ion collisions, *Int. J. Mod. Phys. E* **24**, 1530014 (2015), arXiv:1511.00790 [hep-ph].

[19] Y. Mehtar-Tani, J. G. Milhano, and K. Tywoniuk, Jet physics in heavy-ion collisions, *Int. J. Mod. Phys. A* **28**, 1340013 (2013), arXiv:1302.2579 [hep-ph].

[20] J.-P. Blaizot and Y. Mehtar-Tani, Jet Structure in Heavy Ion Collisions, *Int. J. Mod. Phys. E* **24**, 1530012 (2015), arXiv:1503.05958 [hep-ph].

[21] A. M. Sirunyan *et al.* (CMS), Azimuthal anisotropy of charged particles with transverse momentum up to 100 GeV/ c in PbPb collisions at $\sqrt{s}_{NN}=5.02$ TeV, *Phys. Lett. B* **776**, 195 (2018), arXiv:1702.00630 [hep-ex].

[22] G. Aad *et al.* (ATLAS), Measurement of the Azimuthal Angle Dependence of Inclusive Jet Yields in Pb+Pb Col-

lisions at $\sqrt{s_{NN}} = 2.76$ TeV with the ATLAS detector, Phys. Rev. Lett. **111**, 152301 (2013), arXiv:1306.6469 [hep-ex].

[23] S. Acharya *et al.* (ALICE), Energy dependence and fluctuations of anisotropic flow in Pb-Pb collisions at $\sqrt{s_{NN}} = 5.02$ and 2.76 TeV, JHEP **07**, 103, arXiv:1804.02944 [nucl-ex].

[24] M. Gyulassy, I. Vitev, and X. N. Wang, High p(T) azimuthal asymmetry in noncentral A+A at RHIC, Phys. Rev. Lett. **86**, 2537 (2001), arXiv:nucl-th/0012092.

[25] E. V. Shuryak, The Azimuthal asymmetry at large p(t) seem to be too large for a 'jet quenching', Phys. Rev. C **66**, 027902 (2002), arXiv:nucl-th/0112042.

[26] J. Jia, Azimuthal anisotropy in a jet absorption model with fluctuating initial geometry in heavy ion collisions, Phys. Rev. C **87**, 061901 (2013), arXiv:1203.3265 [nucl-th].

[27] D. Molnar and D. Sun, High-pT suppression and elliptic flow from radiative energy loss with realistic bulk medium expansion, arXiv:1305.1046 [nucl-th] (2013), "eprint".

[28] J. Noronha-Hostler, B. Betz, J. Noronha, and M. Gyulassy, Event-by-event hydrodynamics + jet energy loss: A solution to the $R_{AA} \otimes v_2$ puzzle, Phys. Rev. Lett. **116**, 252301 (2016), arXiv:1602.03788 [nucl-th].

[29] B. Betz, M. Gyulassy, M. Luzum, J. Noronha, J. Noronha-Hostler, I. Portillo, and C. Ratti, Cumulants and nonlinear response of high p_T harmonic flow at $\sqrt{s_{NN}} = 5.02$ TeV, Phys. Rev. C **95**, 044901 (2017), arXiv:1609.05171 [nucl-th].

[30] A. Holtermann, J. Noronha-Hostler, A. M. Sickles, and X. Wang, Measuring jet energy loss fluctuations in the quark-gluon plasma via multiparticle correlations, arXiv:2402.03512 [hep-ph] (2024), "eprint".

[31] L. Barreto, F. M. Canedo, M. G. Munhoz, J. Noronha, and J. Noronha-Hostler, Jet cone radius dependence of RAA and v_2 at PbPb 5.02 TeV from JEWEL+TRENTTo+v-USPhydro, Phys. Lett. B **860**, 139217 (2025), arXiv:2208.02061 [nucl-th].

[32] X. Zhang and J. Liao, Jet Quenching and Its Azimuthal Anisotropy in AA and possibly High Multiplicity pA and dA Collisions, arXiv:1311.5463 [nucl-th] (2013), "eprint".

[33] J. Adam *et al.* (ALICE), Azimuthal anisotropy of charged jet production in $\sqrt{s_{NN}} = 2.76$ TeV Pb-Pb collisions, Phys. Lett. B **753**, 511 (2016), arXiv:1509.07334 [nucl-ex].

[34] V. B. Luong, D. Idrisov, P. Parfenov, A. Taranenko, and A. Demanov, Comparison of methods for elliptic flow measurements at NICA energies SNN=4–11 GeV, AIP Conf. Proc. **2377**, 030011 (2021), arXiv:2103.05064 [nucl-ex].

[35] C. Andres, N. Armesto, H. Niemi, R. Paatelainen, and C. A. Salgado, Jet quenching as a probe of the initial stages in heavy-ion collisions, Phys. Lett. B **803**, 135318 (2020), arXiv:1902.03231 [hep-ph].

[36] D. Zicic, J. Auvinen, I. Salom, M. Djordjevic, and P. Huovinen, Importance of higher harmonics and v4 puzzle in quark-gluon plasma tomography, Phys. Rev. C **106**, 044909 (2022), arXiv:2208.09886 [hep-ph].

[37] D. Zicic, I. Salom, J. Auvinen, P. Huovinen, and M. Djordjevic, DREENA-A framework as a QGP tomography tool, Front. in Phys. **10**, 957019 (2022), arXiv:2110.01544 [nucl-th].

[38] G. Aad *et al.* (ATLAS), Measurements of azimuthal anisotropies of jet production in Pb+Pb collisions at $\sqrt{s_{NN}} = 5.02$ TeV with the ATLAS detector, Phys. Rev. C **105**, 064903 (2022), arXiv:2111.06606 [nucl-ex].

[39] G. Aad *et al.* (ATLAS), Observation of Associated Near-Side and Away-Side Long-Range Correlations in $\sqrt{s_{NN}}=5.02$ TeV Proton-Lead Collisions with the ATLAS Detector, Phys. Rev. Lett. **110**, 182302 (2013), arXiv:1212.5198 [hep-ex].

[40] V. Khachatryan *et al.* (CMS), Observation of Long-Range Near-Side Angular Correlations in Proton-Proton Collisions at the LHC, JHEP **09**, 091, arXiv:1009.4122 [hep-ex].

[41] V. Khachatryan *et al.* (CMS), Evidence for Collective Multiparticle Correlations in p-Pb Collisions, Phys. Rev. Lett. **115**, 012301 (2015), arXiv:1502.05382 [nucl-ex].

[42] B. Abelev *et al.* (ALICE), Long-range angular correlations on the near and away side in p -Pb collisions at $\sqrt{s_{NN}} = 5.02$ TeV, Phys. Lett. B **719**, 29 (2013), arXiv:1212.2001 [nucl-ex].

[43] V. Chekhovsky *et al.* (CMS), Evidence for similar collectivity of high transverse momentum particles in pPb and PbPb collisions, arXiv:2502.07525 [nucl-ex] (2025), eprint.

[44] G. Aad *et al.* (ATLAS), Transverse momentum and process dependent azimuthal anisotropies in $\sqrt{s_{NN}} = 8.16$ TeV p +Pb collisions with the ATLAS detector, Eur. Phys. J. C **80**, 73 (2020), arXiv:1910.13978 [nucl-ex].

[45] C. Aidala *et al.* (PHENIX), Creation of quark-gluon plasma droplets with three distinct geometries, Nature Phys. **15**, 214 (2019), arXiv:1805.02973 [nucl-ex].

[46] M. I. Abdulhamid *et al.* (STAR), Measurements of the Elliptic and Triangular Azimuthal Anisotropies in Central He3+Au, d+Au and p+Au Collisions at $s_{NN}=200$ GeV, Phys. Rev. Lett. **130**, 242301 (2023), arXiv:2210.11352 [nucl-ex].

[47] A. Adare *et al.* (PHENIX), Centrality-dependent modification of jet-production rates in deuteron-gold collisions at $\sqrt{s_{NN}}=200$ GeV, Phys. Rev. Lett. **116**, 122301 (2016), arXiv:1509.04657 [nucl-ex].

[48] U. Acharya *et al.* (PHENIX), Measurement of jet-medium interactions via direct photon-hadron correlations in Au+Au and d +Au collisions at $\sqrt{s_{NN}} = 200$ GeV, Phys. Rev. C **102**, 054910 (2020), arXiv:2005.14270 [hep-ex].

[49] G. Aad *et al.* (ATLAS), Strong Constraints on Jet Quenching in Centrality-Dependent p+Pb Collisions at 5.02 TeV from ATLAS, Phys. Rev. Lett. **131**, 072301 (2023), arXiv:2206.01138 [nucl-ex].

[50] S. Acharya *et al.* (ALICE), Constraints on jet quenching in p-Pb collisions at $\sqrt{s_{NN}} = 5.02$ TeV measured by the event-activity dependence of semi-inclusive hadron-jet distributions, Phys. Lett. B **783**, 95 (2018), arXiv:1712.05603 [nucl-ex].

[51] N. J. Abdulameer *et al.* (PHENIX), Disentangling Centrality Bias and Final-State Effects in the Production of High-pT Neutral Pions Using Direct Photon in d+Au Collisions at $s_{NN}=200$ GeV, Phys. Rev. Lett. **134**, 022302 (2025), arXiv:2303.12899 [nucl-ex].

[52] M. Abdallah *et al.* (STAR), Search for the chiral magnetic effect with isobar collisions at $\sqrt{s_{NN}}=200$ GeV by the STAR Collaboration at the BNL Relativistic Heavy Ion Collider, Phys. Rev. C **105**, 014901 (2022), arXiv:2109.00131 [nucl-ex].

[53] T. Sjostrand, S. Mrenna, and P. Z. Skands, PYTHIA 6.4 Physics and Manual, JHEP **05**, 026,

arXiv:hep-ph/0603175 [hep-ph]%%CITATION = HEP-PH/0603175;%% .

[54] T. Sjostrand, S. Mrenna, and P. Z. Skands, A Brief Introduction to PYTHIA 8.1, *Comput. Phys. Commun.* **178**, 852 (2008), arXiv:0710.3820 [hep-ph]%%CITATION = ARXIV:0710.3820;%% .

[55] C. Hughes, A. C. Oliveira Da Silva, and C. Nattrass, Model studies of fluctuations in the background for jets in heavy ion collisions, *Phys. Rev. C* **106**, 044915 (2022), arXiv:2005.02320 [hep-ph].

[56] T. Mengel, P. Steffanic, C. Hughes, A. C. O. da Silva, and C. Nattrass, Interpretable machine learning methods applied to jet background subtraction in heavy-ion collisions, *Phys. Rev. C* **108**, L021901 (2023), arXiv:2303.08275 [hep-ex].

[57] C. Hughes and T. Mengel, Github: TennGen (2019).

[58] T. Mengel and C. Hughes, Github: tenngen200 (2022).

[59] K. Aamodt *et al.* (ALICE Collaboration), Centrality dependence of the charged-particle multiplicity density at mid-rapidity in Pb-Pb collisions at $\sqrt{s_{NN}} = 2.76$ TeV, *Phys. Rev. Lett.* **106**, 032301. 14 p (2010).

[60] B. Abelev *et al.* (ALICE), Centrality dependence of π , K, p production in Pb-Pb collisions at $\sqrt{s_{NN}} = 2.76$ TeV, *Phys. Rev. C* **88**, 044910 (2013), arXiv:1303.0737 [hep-ex]%%CITATION = ARXIV:1303.0737;%% .

[61] O. Ristea, A. Jipa, C. Ristea, T. Esanu, M. Calin, A. Barzu, A. Scurtu, and I. Abu-Quoad, Study of the freeze-out process in heavy ion collisions at relativistic energies, *Proceedings, 11th International Conference on Nucleus-Nucleus Collisions (NN2012): San Antonio, Texas, May 27-June 1, 2012*, *J. Phys. Conf. Ser.* **420**, 012041 (2013)%%CITATION = 00462,420,012041;%% .

[62] E. Schnedermann, J. Sollfrank, and U. W. Heinz, Thermal phenomenology of hadrons from 200-A/GeV S+S collisions, *Phys. Rev. C* **48**, 2462 (1993), arXiv:nucl-th/9307020.

[63] A. Adare *et al.* (PHENIX), Measurement of the higher-order anisotropic flow coefficients for identified hadrons in Au+Au collisions at $\sqrt{s_{NN}} = 200$ GeV, *Phys. Rev. C* **93**, 051902 (2016), arXiv:1412.1038 [nucl-ex].

[64] J. Adam *et al.* (ALICE), Higher harmonic flow coefficients of identified hadrons in Pb-Pb collisions at $\sqrt{s_{NN}} = 2.76$ TeV, *JHEP* **09**, 164, arXiv:1606.06057 [nucl-ex]%%CITATION = ARXIV:1606.06057;%% .

[65] P. Skands, S. Carrazza, and J. Rojo, Tuning PYTHIA 8.1: the Monash 2013 Tune, *Eur. Phys. J. C* **74**, 3024 (2014), arXiv:1404.5630 [hep-ph].

[66] M. Cacciari, G. P. Salam, and G. Soyez, FastJet User Manual, *Eur. Phys. J. C* **72**, 1896 (2012), arXiv:1111.6097 [hep-ph].

[67] P. Steffanic, C. Hughes, and C. Nattrass, Separating signal from combinatorial jets in a high-background environment, *Phys. Rev. C* **108**, 024909 (2023), arXiv:2301.09148 [hep-ph].

[68] A. Bilandzic, R. Snellings, and S. Voloshin, Flow analysis with cumulants: Direct calculations, *Phys. Rev. C* **83**, 044913 (2011), arXiv:1010.0233 [nucl-ex].

[69] J. Jia, M. Zhou, and A. Trzupek, Revealing long-range multiparticle collectivity in small collision systems via subevent cumulants, *Phys. Rev. C* **96**, 034906 (2017), arXiv:1701.03830 [nucl-th].

[70] G. D'Agostini, A multidimensional unfolding method based on bayes' theorem, *Nuclear Instruments and Methods in Physics Research Section A: Accelerators, Spectrometers, Detectors and Associated Equipment* **362**, 487 (1995).

[71] L. Brenner, R. Balasubramanian, C. Burgard, W. Verkerke, G. Cowan, P. Verschuur, and V. Croft, Comparison of unfolding methods using RooFitUnfold, *Int. J. Mod. Phys. A* **35**, 2050145 (2020), arXiv:1910.14654 [physics.data-an].

[72] R. A. Lacey, The Role of elliptic flow correlations in the discovery of the sQGP at RHIC, *Proceedings, 18th International Conference on Ultra-Relativistic Nucleus-Nucleus Collisions (Quark Matter 2005): Budapest, Hungary, August 4-9, 2005*, *Nucl. Phys.* **A774**, 199 (2006), arXiv:nucl-ex/0510029 [nucl-ex]%%CITATION = NUCL-EX/0510029;%% .

[73] N. Borghini, P. M. Dinh, and J.-Y. Ollitrault, Are flow measurements at SPS reliable?, *Phys. Rev. C* **62**, 034902 (2000), arXiv:nucl-th/0004026 [nucl-th]%%CITATION = NUCL-TH/0004026;%% .

[74] M. Luzum and J.-Y. Ollitrault, Directed flow at midrapidity in heavy-ion collisions, *Phys. Rev. Lett.* **106**, 102301 (2011), arXiv:1011.6361 [nucl-ex]%%CITATION = ARXIV:1011.6361;%% .

[75] E. Retinskaya, M. Luzum, and J.-Y. Ollitrault, Directed flow at midrapidity in $\sqrt{s_{NN}} = 2.76$ TeV Pb+Pb collisions, *Phys. Rev. Lett.* **108**, 252302 (2012), arXiv:1203.0931 [nucl-th]%%CITATION = ARXIV:1203.0931;%% .

[76] G. Aad *et al.* (ATLAS), Measurement of the azimuthal anisotropy for charged particle production in $\sqrt{s_{NN}} = 2.76$ TeV lead-lead collisions with the ATLAS detector, *Phys. Rev. C* **86**, 014907 (2012), arXiv:1203.3087 [hep-ex]%%CITATION = ARXIV:1203.3087;%% .

[77] X.-l. Zhu, M. Bleicher, and H. Stoecker, Elliptic flow analysis at RHIC: Fluctuations vs. non-flow effects, *Phys. Rev. C* **72**, 064911 (2005), arXiv:nucl-th/0509081.